THE ASTROPHYSICAL JOURNAL, 481:578–586, 1997 June 1

CLUSTERING OF GALAXIES IN THE HUBBLE DEEP FIELD

JENS V. VILLUMSEN
Max-Planck-Institut für Astrophysik, Karl-Schwarzschild-Strasse 1, D-85740 Garching, Germany
WOLFRAM FREUDLING
Space Telescope European Coordinating Facility and European Southern Observatory, Karl-Schwarzschild-Strasse 2, D-85748 Garching, Germany
AND
LUIZ N. DA COSTA
European Southern Observatory, Karl-Schwarzschild-Strasse 2, D-85748 Garching, Germany; and Observatório Nacional, rua General José Cristino 77, Rio de Janeiro, Brazil
Received 1996 June 11; accepted 1996 November 19

ABSTRACT

We compute the two-point angular correlation function $w(\theta)$ for a sample of ~ 1700 galaxies to a magnitude limit equivalent to $R \sim 29.5$, using a catalog derived from the Hubble Deep Field images. A nonzero value of $w(\theta)$ is measured down to $R = 29.0$. The amplitude of $w(\theta)$ at the bright magnitude limit ($R \sim 26$) is consistent with previous ground-based observations. At fainter magnitudes the clustering amplitude continues to decrease, but at a slower rate than that predicted by the power law $w(1'') \propto 10^{-0.27R}$ observed for shallower samples. The observed $w(\theta)$ over the magnitude range $20 < R < 29$ is consistent with linear evolution of the clustering of a galaxy population which at present has a correlation length r_0 of about 4 h^{-1} Mpc, close to that of local *IRAS* galaxies. We also investigate the impact that magnification bias induced by weak gravitational lensing may have on our results. Although the observed amplitude of $w(\theta)$ can differ from the true amplitude by up to 30%, this effect is not large enough to influence our conclusions. Finally, by using a color-selected sample, we examine whether the expected effects of magnification bias can be used for an independent determination of cosmological parameters in deep images. We conclude that the amplitude of the effect can be large and in some cases even produce an upturn of the amplitude of the correlation with limiting magnitude. However, we find that it is not possible to detect the effects of magnification bias on $w(\theta)$ from images alone. If redshift information becomes available, it is possible to measure the effects of magnification bias directly and thus constrain the density parameter Ω_0 and the bias factor b.

Subject headings: cosmology: observations — galaxies: clusters: general — large-scale structure of universe

1. INTRODUCTION

An important constraint on the formation and evolution of structures in the universe is the three-dimensional two-point correlation function $\xi(r)$ as a function of redshift z. Unfortunately, redshift surveys to measure the intrinsic clustering properties of faint galaxies ($R \gtrsim 25.5$), presumably at high redshifts ($z \gtrsim 1$), are difficult even with the new generation of large-aperture telescopes. Such direct measurements of $\xi(r)$ for $z \sim 1$ are only now becoming available (e.g., Cole et al. 1994; Le Fèvre et al. 1996). Therefore, to study the clustering properties of faint galaxies, one must for now rely on studies of the angular two-point correlation function $w(\theta)$. Some constraints on the redshift dependence of $\xi(r)$ can be obtained by investigating the dependence of the amplitude of $w(\theta)$ on the limiting magnitude.

Recent studies of $w(\theta)$ have pushed the limiting magnitude to ever fainter flux levels. Current observational limits reach $R = 26$ (e.g., Brainerd, Smail, & Mould 1995, hereafter BSM). There is general agreement that the amplitude of $w(\theta)$ decreases more rapidly with limiting magnitude than expected from a redshift distribution $N(z)$ as predicted by "no-evolution models" and linear evolution of the clustering. However, the interpretation of these observations depends on the assumed model for the redshift distribution and clustering evolution, which are both poorly constrained by current data (e.g., Glazebrook et al. 1995; Le Fèvre et al. 1996). Some authors have argued that good agreement with the data can be obtained with models that assume modest clustering evolution of locally observed low surface brightness galaxies (BSM).

Extending the analysis to fainter magnitudes is of great interest in order to impose more stringent constraints on the epoch of formation of structures. However, as first pointed out by Villumsen (1996, hereafter V96), the interpretation of such data needs to take into account the effect of magnification bias induced by weak gravitational lensing, which may affect the measurement of $w(\theta)$ at faint magnitudes. As discussed by V96, this effect is expected to be important for samples with a median redshift $\gtrsim 1$, and it may therefore affect the analysis of very deep galaxy samples such as those extracted from the Hubble Deep Field (HDF; Williams et al. 1996). The effect should be most evident in samples that preferentially include "red" galaxies and therefore have shallow number count slopes (Broadhurst 1996). A possible signature of the effect would be an upturn of the correlation amplitude with the median redshift of the sample, which should correlate with the magnitude limit.

The detection of magnification bias could be an important tool to further constrain cosmological models. The amplitude of this effect is a measurement of the clustering of the mass and depends on the product $\Omega_0 \sigma_8$, where Ω_0 is the cosmological density parameter and σ_8^2 is the variance of the *mass* fluctuations within a sphere 8 h^{-1} Mpc in radius.

Therefore, the behavior of the clustering amplitude as a function of the limiting magnitude could provide a test of the value of the product $\Omega_0\sigma_8$.

In this paper we use the HDF to investigate the behavior of the amplitude of $w(\theta)$ with magnitude reaching at least 3 mag fainter than published data from ground-based observations. The faint-magnitude limit and the color information make these data ideal, except for the small angular coverage, to investigate the behavior of $w(\theta)$ at faint flux levels and the contribution of magnification bias to the observed clustering of faint galaxies. Previous work on galaxy clustering in the HDF field has been carried out by Colley et al. (1996), focusing on very small angular scales and discussing the possible existence of subgalactic clumps at high redshift. Here, instead, we use the HDF data to investigate the evolution of $\xi(r)$ as a function of redshift.

In § 2 we describe the catalog used in the analysis. In § 3 we predict the correlation function $w(\theta)$ in the absence of magnification bias for simple models of the redshift distribution and clustering evolution. In § 4 we compute the two-point angular correlation function for different magnitude-limited samples and determine the variation of the clustering amplitude as a function of the magnitude limit. Section 5 describes the theoretical calculation of the effects of magnification bias on $w(\theta)$, and compares the modified curves with the data. In § 6 the same analysis is done for a color-selected sample, which should be more sensitive to the effects of the magnification bias. Our conclusions are summarized in § 7.

2. THE GALAXY CATALOG

Williams et al. (1996) presented a catalog of galaxies extracted from the HDF images with FOCAS. An alternative galaxy catalog has been used by Clements & Couch (1996). This catalog, which was generated using the SExtractor program (Bertin & Arnouts 1995), was kindly provided to us by Couch (1996). As pointed out by Williams et al. (1996), the FOCAS catalog finds in a significant number of cases several objects where visual inspection of the images indicates that there is only a single galaxy. A comparison of the two catalogs with the HDF images leads us to believe that Couch's catalog contains a smaller number of such cases. For this reason we used that catalog for this work. A minimum object extraction area of 30 pixels and a detection threshold of 1.3 σ above the background were used. The magnitudes were computed with the zero points given by Holtzman et al. (1996). For this work, we used the catalogs extracted from the images taken with the F606W filter, which is similar to an R passband, and the F814W filter, which corresponds to the I band. Since only a very small number of stars is expected in the HDF field, we did not attempt to use the galaxy/star separation parameter given by the SExtractor program, and treated all detected objects as galaxies. In order to avoid edge problems, only galaxies with pixel coordinates in the range $250 < x, y < 2050$ were used. The total of 1732 galaxies detected in the F606W filter were used, out of which 1256 were detected in both the F606W and the F814W filters. Hereafter, we refer to the two bands as R and I, respectively.

3. PREDICTED CORRELATION FUNCTION

The method to derive the angular correlation function from the intrinsic correlation function (neglecting magnification bias) for a given redshift distribution is well known (e.g., Peebles 1980). Following Efstathiou et al. (1991), we assume that the evolution of the intrinsic correlation function is given by

$$\xi(r, z) = \left(\frac{r}{r_0}\right)^{-\gamma}(1+z)^{-(3+\epsilon)}, \quad \gamma = 1.8, \tag{1}$$

when expressed in proper coordinates. A power index $\epsilon = 0.8$ corresponds to linear evolution of the correlation function, while $\epsilon = 0$ corresponds to a correlation function constant in proper coordinates. Here r_0 is the present-day correlation length.

We adopt the redshift distribution

$$N(z) = \frac{\beta z^2}{z_0^3\,\Gamma[3/\beta]}\exp\left[-\left(\frac{z}{z_0}\right)^{\beta}\right], \quad \beta = 2.5, \tag{2}$$

where z_0 is approximately the median redshift (e.g., Efstathiou et al. 1991) and Γ is the gamma function. Values for z_0 were provided by Charlot (1996). The adopted redshift distribution predicts that for a magnitude limit of $R = 28$, 84% of the galaxies are at $z > 1$ and 29% of the galaxies at $z > 2$. Given the uncertainties, these estimates are in reasonable agreement with the estimated redshift distribution based on photometric redshifts from HDF (Mobasher et al. 1996). It is important to note that the redshift distribution and hence the median redshifts are quite uncertain for faint, magnitude-limited samples such as the one considered here. This is probably the largest uncertainty in inferring the amplitude and evolution of $\xi(r, z)$ from the present sample.

With this parameterization, we can calculate $w(\theta)$ using Limber's equation (e.g., Efstathiou et al. 1991)

$$\omega(\theta) = \pi^{1/2}\,\frac{\Gamma[(\gamma-1)/2]}{\Gamma[\gamma/2]}\,r_0^{\gamma}\,\theta^{1-\gamma} \times \int_0^{\infty} dz\,H(z)N^2(z)x^{1-\gamma}(1+z)^{\gamma-3-\epsilon}. \tag{3}$$

Here $H(z)$ is the Hubble constant as a function of redshift, normalized so that $H(z=0) \equiv 1$, and $x(z) = 2[1-(1+z)^{-1/2}]$ is the comoving angular diameter distance. Since the results for the observed correlation function depend only weakly on Ω_0 (BSM), we assume hereafter that $\Omega_0 = 1$.

4. CORRELATION FUNCTION FROM THE HDF CATALOG

We have extracted from our catalog eight R-magnitude–limited samples with magnitude limits ranging from $R = 26.0$ to $R = 29.5$ in 0.5 mag steps, discarding all galaxies brighter than $R = 23$. Although the samples as defined are not totally independent, they are nearly so because the sample size increases rapidly with limiting magnitude.

The angular correlation function $w(\theta)$ is estimated using the estimator described by Landy & Szalay (1993) and BSM:

$$w(\theta) = \frac{\mathrm{DD} - 2\mathrm{DR} + \mathrm{RR}}{\mathrm{RR}}. \tag{4}$$

Here DD, DR, and RR are the number of data-data, data-random, and random-random pairs at a given angular separation.

For each magnitude limit we generated a random sample within the same region of the galaxy catalog but with 5

times as many objects. The number of DR and RR pairs are scaled to the number of DD pairs. The angular correlation function $w(\theta)$ for each magnitude limit was estimated from pairs of galaxies with angular separations in the range $2'' < \theta < 80''$. The total number of pairs at a given separation was calculated by summing the number of pairs at the corresponding separation within each individual chip. Pairs across chip boundaries were excluded in order to minimize additional uncertainties associated with chip-to-chip variations of the photometric zero point. The finite number of galaxies in the random samples adds an uncertainty to the observed correlation function. However, this uncertainty is far smaller than the uncertainty due to the finite number of real galaxies. A recalculation of $w(\theta)$ with 10 times as many random galaxies as real galaxies leads to the same result. As a consistency check, we have also estimated $w(\theta)$ from counts in cells, and the results are similar to those shown here.

Errors were estimated both from Poisson statistics and from 30 bootstrap resamples of the data (see, e.g., Barrow, Sonoda, & Bhavsar 1984). Both error estimates agree well at large separations. Fits to the correlation function are not sensitive to the differences between the error estimates at small scales. The errors estimated from the bootstrap resampling are consistent with the field-to-field variations of $w(\theta)$ as measured for the three chips.

Due to the small angular size of the chips, it is necessary to take into account the "integral constraint." The background density of galaxies is estimated from the sample itself, forcing the integral of the correlation function over the survey area to be zero. Since the angular size of the survey area is small, $w(\theta)$ is reduced by the amount

$$C \equiv \frac{1}{\Omega^2} \iint d\Omega_1 \, d\Omega_2 \, w(\theta) \, , \tag{5}$$

the so-called integral constraint (BSM). Here Ω is the solid angle of the survey area on the sky. If we assume that $w(\theta)$ is a power law,

$$w(\theta) = A\theta^{-\gamma+1} \, , \quad \gamma = 1.8 \, , \tag{6}$$

then $C = 0.071A$ for our survey geometry for θ measured in arcseconds.

Figure 1 shows the observed $w(\theta)$ for the eight magnitude limits. We determined the amplitude of $w(\theta)$ by fitting

$$w(\theta) = A\theta^{-\gamma+1} - C \, , \quad \gamma = 1.8 \, , \tag{7}$$

which takes into account the integral constraint. These fits are shown as solid lines in Figure 1. The data points at different angular separations are correlated, but this is ignored in the fit. The error bars represent 1 σ Poisson errors. There are two possible systematic effects that may

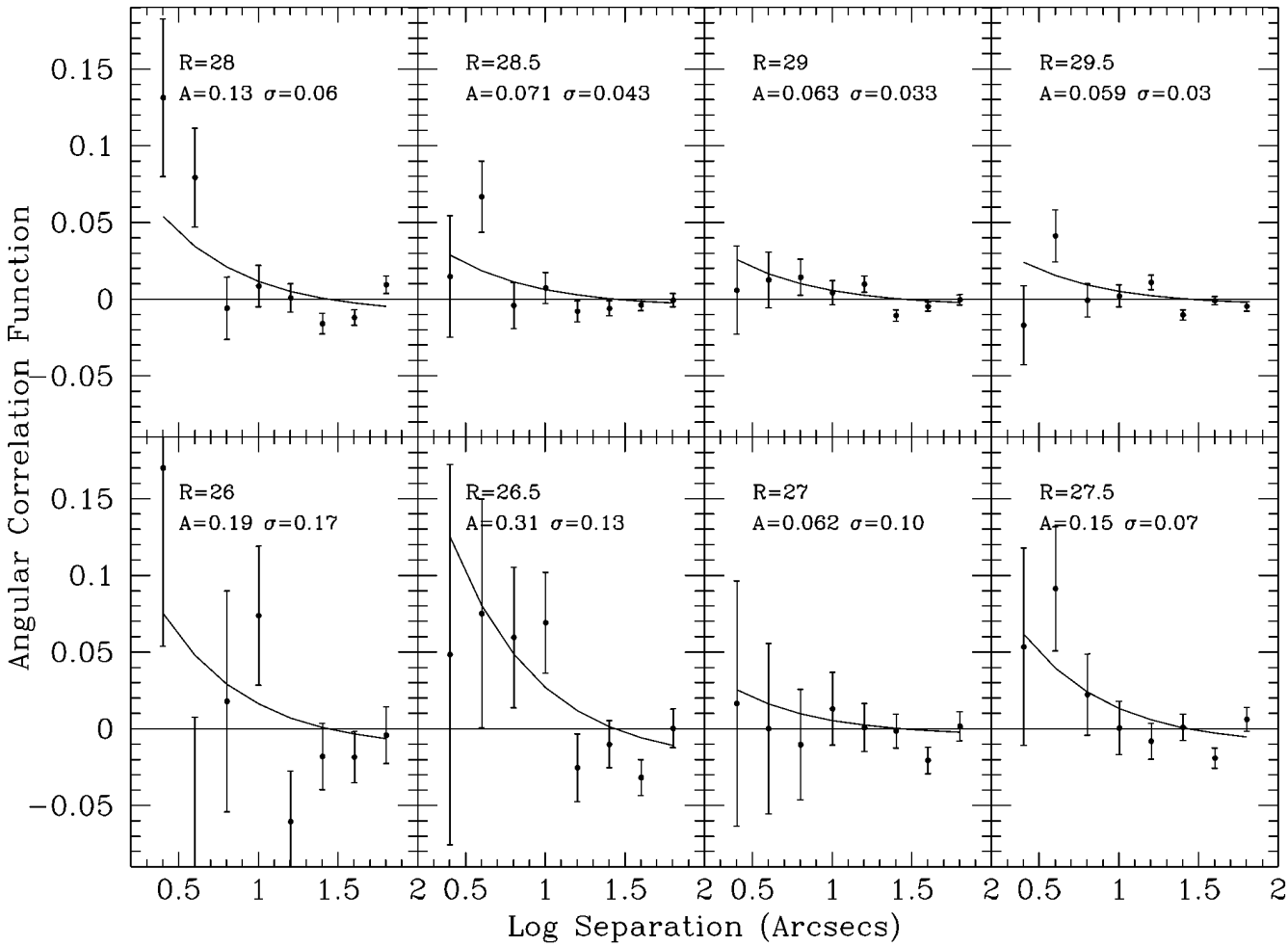

FIG. 1.—Measured $w(\theta)$ for all galaxies brighter than the limiting magnitude R as indicated in each panel. Error bars represent the 1 σ Poisson errors. The solid lines are the best fits for fixed power-law index $\gamma = 1.8$. The integral constraint (see text) has been included in the fits.

affect our $w(\theta)$ estimates. The first is due to merging of images, especially at fainter magnitudes. This effect should not be important in our calculations, as it will preferentially affect $w(\theta)$ on very small angular scales that have little weight in our fits to the data.

A second potential effect is due to the incompleteness of the galaxy sample close to the magnitude limit of the HDF data. Although there is no detailed study of the incompleteness of the HDF galaxy sample, the behavior of the number counts down to $R \sim 29$ indicates that incompleteness should not be important at brighter magnitudes. Moreover, the conclusions presented below would not change if we considered only galaxies brighter than $R \sim 28$, which is 1 mag brighter than the magnitude at which we may reasonably expect the onset of incompleteness effects.

We have applied Kendall's τ-test to estimate the significance level at which the null hypothesis of zero signal can be rejected. We find that the significance of the detection is greater than 2 σ for all subsamples except the brightest, presumably because the small number of galaxies, and the faintest, possibly because of the incompleteness of the sample. In Table 1 we summarize the observational results. Columns (1)–(5) give the magnitude limits, the estimate of the median redshift, the number of galaxies in the sample, the amplitude of $w(\theta)$ at 1″, and the associated 1 σ error.

Figure 2 shows the amplitudes of the correlation function as derived from the fits of Figure 1 as a function of magnitude limit, scaled to a separation of 1″. The filled circles are the HDF data, and the error bars are 1 σ uncertainties from fitting equation (7) to the measured correlation function. The open circles are the data taken from BSM but converted to the amplitude at 1″. The figure includes data from Couch, Jurcevic, & Boyle (1993), Efstathiou et al. (1991), Roche et al. (1993), and Stevenson et al. (1985), in addition to the BSM data points.

The results of the HDF data are consistent with those of BSM at bright magnitudes, despite the admittedly large error bars. However, at fainter limits the clustering amplitude falls off slower than the power law $A(R) \propto 10^{-0.27R}$ proposed by BSM to fit the data at brighter magnitudes in the range $18 < R < 25$. Although all HDF points lie well above this line, there is no indication of an upturn at very faint magnitudes as previously claimed by different authors in the B band (e.g., Neuschaefer, Windhorst, & Dressler 1991; Landy, Szalay, & Koo 1996).

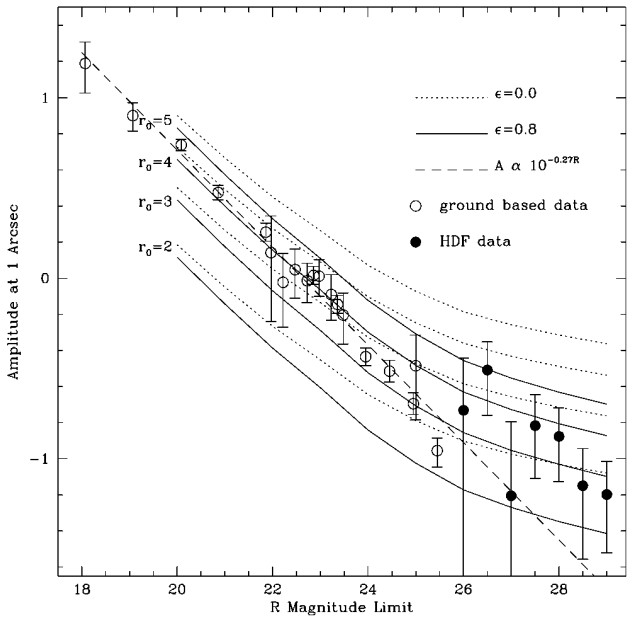

FIG. 2.—Observed amplitude of $w(\theta)$, measured at 1″ separation as a function of limiting R magnitude, for $18 < R < 29$. Points plotted as filled circles are from HDF data, and those plotted as open circles are adapted from Fig. 2 of BSM, including 1 σ error bars. The dashed line is a power-law fit to the data from BSM. The curves are theoretical predictions assuming $N(z)$ as described in the text for different values of the present correlation lengths r_0 as indicated, with the amplitude increasing with the adopted r_0. The dotted curves are for $\epsilon = 0$, while the solid curves are for $\epsilon = 0.8$.

The curves in Figure 2 are theoretical predictions of the amplitude of $w(\theta)$ assuming a redshift distribution given by equation (2), using values for the median redshift as listed in Table 1. We have considered models with $\epsilon = 0$ and 0.8, and $r_0 = 2$–$5\ h^{-1}$ Mpc in $1\ h^{-1}$ Mpc steps. The dotted curves are the predictions for a local galaxy population with different correlation lengths r_0 and $\epsilon = 0$, while the solid curves are the predictions for $\epsilon = 0.8$. The theoretical curves predict that the correlation amplitude will decrease slower

TABLE 1

OBSERVED CORRELATION FUNCTIONS

		FULL SAMPLE			RED SAMPLE		
MAGNITUDE LIMIT (1)	REDSHIFT ESTIMATE (2)	Number of Galaxies (3)	Amplitude (4)	Error (5)	Number of Galaxies (6)	Amplitude (7)	Error (8)
20.0	0.25	...	...	...	...	...	...
21.0	0.35	...	...	...	...	...	...
22.0	0.48	...	...	...	...	...	...
23.0	0.64	...	...	...	...	...	...
24.0	0.87	...	...	...	...	...	...
25.0	1.11	...	...	...	...	...	...
26.0	1.35	263	0.19	0.18	249	0.35	0.19
26.5	...	384	0.31	0.14	362	0.30	0.15
27.0	1.54	536	0.06	0.10	510	0.10	0.10
27.5	...	692	0.15	0.07	655	0.08	0.08
28.0	1.71	900	0.13	0.06	839	0.13	0.06
28.5	...	1230	0.071	0.043	1082	0.073	0.049
29.0	1.87	1559	0.063	0.033	1226	0.057	0.043
29.5	...	1732	0.059	0.030	1256	0.043	0.041

than the power law observed at brighter magnitudes, consistent with our data.

A model with linear evolution of the clustering amplitude ($\epsilon = 0.8$) with a present- day correlation length $r_0 \approx 4\ h^{-1}$ Mpc fits the data remarkably well over a range of nine magnitudes, $20 \lesssim R \lesssim 29$. This value of r_0 is very similar to that measured for *IRAS* galaxies (Fisher et al. 1994), consistent with the picture that faint HDF and present-day *IRAS* galaxies are drawn from the same population of field galaxies. If this is true, it would suggest that *IRAS* galaxies were formed at redshifts $z \gtrsim 1.5$. As pointed out above, these conclusions depend critically on the assumed redshift distribution and must await supporting evidence.

This conclusion contrasts with that of BSM, who argue in favor of a very weakly clustered population with $r_0 \approx 2\ h^{-1}$ Mpc, presumably low surface brightness galaxies, or the interpretation of Landy et al. (1996) for a low-redshift population of very faint, weakly clustered blue galaxies. The reason for this discrepancy is that we have assumed a higher median redshift, which is supported by the results of Mobasher et al. (1996). At faint magnitudes, the HDF data can also be fitted with a model with slow evolution, i.e., $\epsilon = 0$, if $r_0 = 2$–$3\ h^{-1}$ Mpc. However, such a model would be inconsistent with the data for $R \lesssim 25$, being too shallow at brighter magnitudes.

Since we have assumed that the median redshift of galaxies in HDF is larger than unity, the effects of weak gravitational lensing can influence the observed correlation function of galaxies. This so-called magnification bias could in principle affect our conclusion (V96). The importance of this effect for the HDF sample is evaluated in the next section.

5. EFFECTS OF MAGNIFICATION BIAS

V96 has shown that the magnification bias can have a significant influence on $w(\theta)$ provided that (1) the sample depth in redshift is $z \gtrsim 1$; (2) the slope s of the number counts is significantly different from 0.4; and (3) the quantity $\Omega_0\,\sigma_8$ is not much less than unity. We emphasize that σ_8 is the rms mass density fluctuation on a scale of $8\ h^{-1}$ Mpc.

The magnification bias, as shown by Broadhurst, Taylor & Peacock (1995), will affect the number density of galaxies at a given position on the sky. If the slope of the number counts is s and the magnification due to gravitational lensing from a matter overdensity is μ, then the observed number density $N_{\rm obs}$ of background objects will be different from the "true" number density $N_{\rm true}$ of objects

$$N_{\rm obs} = N_{\rm true}\,\mu^{2.5s-1}\ . \tag{8}$$

Note that $\mu = 1$ corresponds to no magnification. Assuming there are no intrinsic correlations of galaxies, then apart from random fluctuations due to the finite number of galaxies, the number density of galaxies is constant across the sky. In the presence of mass density fluctuations, gravitational lensing will change the number density of galaxies according to equation (8). The amplification will be a function of position in the sky, and therefore the number density of galaxies will be a function of position. This means that a nonzero correlation amplitude is observed even in the absence of intrinsic galaxy clustering. In the limit of weak clustering, i.e., $|\,\mu - 1\,| \ll 1$, the magnification μ relates to the "convergence" κ as $\mu = 1 + 2\kappa$ (e.g., Blandford et al. 1991; Broadhurst et al. 1995). The quantity κ is a dimensionless measure of the surface mass overdensity. If the intrinsic relative overdensity is $\Delta\mu$, we find that

$$N_{\rm obs} = N_0[1 + \Delta\mu + (5s - 2)\kappa]\ . \tag{9}$$

Here N_0 is the average number density of galaxies, so that $N_{\rm true} = N_0(1 + \Delta\mu)$, and $N_{\rm obs}$ is the observed number density of galaxies. Since we assume that the clustering and the lensing are both weak, the clustering term $\Delta\mu$ and the lensing term $(5s - 2)\kappa$ are additive, and we get an observed correlation function

$$w(\theta) \equiv \left\langle \frac{N_{\rm obs}(\boldsymbol{\theta}_0)N_{\rm obs}(\boldsymbol{\theta}_0 + \boldsymbol{\theta})}{N_0^2} - 1 \right\rangle$$
$$\equiv \omega_{\rm gg}(\theta) + (5s - 2)^2\omega_{\kappa\kappa}(\theta) + 2(5s - 2)\omega_{\rm g\kappa}(\theta)\ . \tag{10}$$

The angular brackets denote a directional average. It can be seen that there are three terms to the observed correlation function. The first term is due to the true clustering of galaxies, the second term is due to the mass density fluctuations, while the last is a cross term. For details of the calculation of the effects of gravitational lensing see V96.

In order to evaluate the importance of magnification bias, we compare the two terms in equation (9) on a scale of 5′. The rms density fluctuation on that scale is approximately 0.035 for the sample $R < 25.5$ (BSM). If the redshift of that sample is $z \sim 1$, then the rms κ smoothed on the same scale is $\sigma_\kappa \approx 0.015\Omega_0\,\sigma_8$. If $s = 0.3$, then the lensing term in equation (9) will be approximately $(5s - 2)\kappa \approx 0.008$ for $\Omega_0\,\sigma_8 = 1$. This is not negligible compared to the intrinsic clustering term unless $\Omega_0\,\sigma_8 \ll 1$. If our galaxy sample has a number-count slope of $s = 0.2$, we greatly increase the effect of lensing. In that case, the lensing term $(5s - 2)\kappa$ will double to ≈ 0.016. Therefore, $w(\theta)$ can be significantly influenced by magnification bias as shown in Figure 1 of V96. In that paper the effect was evaluated in terms of the median redshift of the sample.

For a given set of cosmological parameters, such as Ω_0, Λ, σ_8, and intrinsic galaxy-galaxy $\xi_{\rm gg}(r, z)$ and mass-mass $\xi_{\rm mm}(r, z)$ correlation functions, we can calculate $\omega_{\rm gg}(\theta)$ and $(5s - 2)^2\omega_{\kappa\kappa}(\theta)$ for an observed redshift distribution $N(z)$ of galaxies. In order to calculate $2(5s - 2)\omega_{\rm g\kappa}(\theta)$, it is necessary to compute the galaxy-mass $\xi_{\rm gm}(r, z)$ correlation function, or, in other words, the relation between the galaxy and mass distributions. If there is no correlation, then $\omega_{\rm g\kappa}$ is by definition zero. The next simplest assumption is the linear bias model, whereby the galaxy overdensity equals the mass overdensity apart from a factor b. This is the model we use for theoretical predictions,

$$\xi_{\rm gm}(r, z) = b\xi_{\rm mm}(r, z)\ , \quad \xi_{\rm gg}(r, z) = b^2\xi_{\rm mm}(r, z)\ , \tag{11}$$

where b is the biasing factor. In the linear bias model we then get (V96)

$$(\theta) = \pi^{1/2}\,\frac{\Gamma[(\gamma - 1)/2]}{\Gamma[\gamma/2]}\,r_0^\gamma\,\theta^{1-\gamma}\int_0^\infty dz \tag{12}$$
$$\times \left\{H(z)\left[N(z) + 3\,\frac{\Omega_0}{b}\,(5s - 2)\phi(z)y(z)(1 + z)H^{-1}(z)\right]^2\right.$$
$$\left.\times\, x(z)^{1-\gamma}(1 + z)^{\gamma-3-\epsilon}\right\}. \tag{13}$$

This is a generalization of equation (3). Here $x(z)$ and $y(z)$ are the comoving radial and angular diameter distances, and $\phi(z)$ is the lensing selection function which is the inte-

gral over all sources more distant than z of the ratio of the comoving angular lens-source distance $y_{LS}(z', z)$ and observer-source distance $y_{OS}(z)$

$$\phi(z') = \int_{z'}^{\infty} dz\, N(z)\, \frac{y_{LS}(z', z)}{y_{OS}(z)} . \quad (14)$$

As stated in V96, the cosmological constant Λ has little influence on weak gravitational lensing and therefore magnification bias. In equation (13) the dependence of $w(\theta)$ on the rms mass density fluctuations parameterized by σ_8 has been expressed in terms of the galaxy correlation length r_0 and the bias factor b for a particular galaxy population, using the linear bias model.

The contribution to $w(\theta)$ from gravitational lensing depends on the product $\Omega_0 \times \sigma_8$. For the cross term, the dependence is linear and for the pure lensing term the dependence is quadratic. In this paper we have performed all calculations for a model in which $\Omega_0 = 1$, $\Lambda = 0$ and for various values of σ_8. We note that for a fixed value of r_0, a scaling in σ_8 is equivalent to a scaling in b.

In Figure 3 we show the theoretical predictions for the correlation amplitude including the effects of magnification bias. The slope of the number counts in the R band is measured to be $s = 0.31 \pm 0.03$, consistent with results from brighter samples (Smail et al. 1995). The observed data points are shown in the two panels of Figure 3 together with the theoretical predictions both with and without magnification bias. In the left panel we assume that $\epsilon = 0$ and show the predictions for the amplitude for $\sigma_8 = 0.5$, i.e., a highly biased model (*long-dashed curve*) and for $\sigma_8 = 1$ (*short-dashed curve*), i.e., an unbiased model. In the right panel it is assumed that $\epsilon = 0.8$.

These theoretical curves can be compared with the curves in Figure 1 of V96. In that paper, the effects of magnification bias are shown in terms of median redshift, while here we show the effects in terms of limiting magnitude, which is an observable.

The basic effect of magnification bias is to decrease the observed amplitude of clustering. It is larger for small values of r_0 and larger values of ϵ. The effects of magnification bias are also increasing functions of limiting magnitude. These effects can be simply understood in terms of a competition between the effects of true clustering and the clustering induced by the magnification bias. The intrinsic clustering contribution decreases with decreasing value of r_0 and increasing values of ϵ and limiting magnitude. The clustering contribution from magnification bias is an increasing function of σ_8 and limiting magnitude. From the figure, we find that the decrease in amplitude is in the range 10%–25% and is not very sensitive to the limiting magnitude. The amplitude is already high at a magnitude limit $R \sim 25$, which corresponds to the spectroscopic limit of large telescopes. As discussed below, this fact provides us with a possible way of directly measuring the magnification bias and therefore $\Omega_0\sigma_8$ in deep redshift surveys. Even though the effects of magnification bias are not negligible, they are not large enough to change the conclusions in § 4.

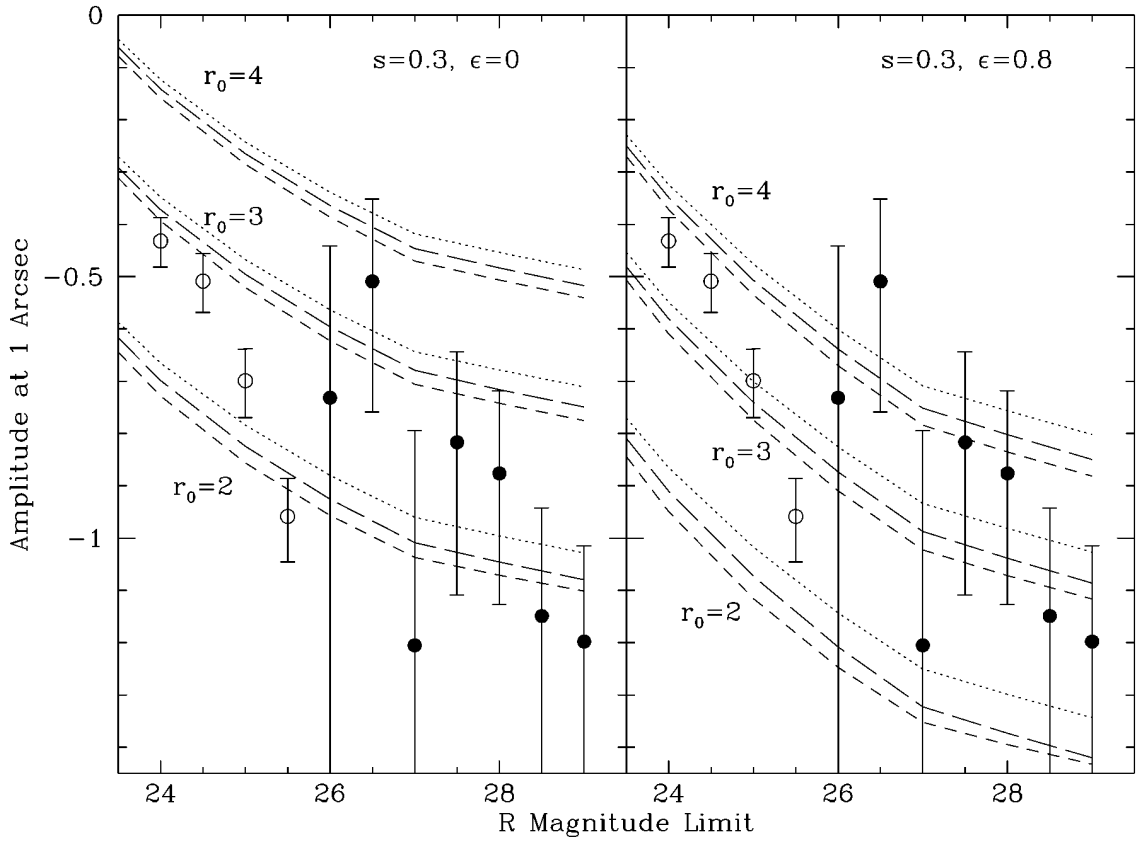

FIG. 3.—Observed amplitude of $w(\theta)$, measured at 1″ separation as a function of limiting R magnitude, for $24 < R < 29$. Points plotted as filled circles are from HDF data, and those plotted as open circles are from BSM data. The curves are theoretical predictions assuming $N(z)$ as described in the text for different values of the present correlation lengths r_0 as indicated. In the left-hand panel $\epsilon = 0$ is assumed, while in the right-hand panel $\epsilon = 0.8$ is assumed. The dotted curves are predictions without the effects of magnification bias. The dashed curves are equivalent curves including the effects of magnification bias. The long-dashed curves are for $\sigma_8 = 0.5$, and the short-dashed curves are for $\sigma_8 = 1$. The observed number-count slope $s = 0.3$ is used in the predictions.

In our analysis we have considered only the effect of magnification bias caused by large-scale structure. Weak lensing by individual galaxy halos, i.e., galaxy-galaxy lensing (e.g., Brainerd, Blandford, & Smail 1996) can change the correlation function on small angular scales through the magnification bias. Given the uncertainty in the size and masses of galaxy halos, the magnitude of this effect is uncertain. However, judging by the results of Brainerd et al. (1996), which reported a weak detection of the effect, it is unlikely that this effect will make a significant contribution to $w(\theta)$.

The reason the effects of magnification bias are not more noticeable is that there is a large fraction of low-redshift galaxies in the sample for which magnification bias is not important. Furthermore, the full sample considered so far has a number-count slope $s \approx 0.3$, close to the neutral slope $s = 0.4$. This motivates us to look for a subsample for which the number-count slope is significantly lower than 0.3.

6. MAGNIFICATION BIAS FOR A COLOR-SELECTED SAMPLE

It is clear from equation (10) that the effects of magnification bias are larger if the number-count slope, s, for the sample considered is significantly different from 0.4. In particular, V96 has shown that for a sample with $s = 0.2$, magnification bias can produce a distinctive upturn in the amplitude of $w(\theta)$ for samples with median redshifts $z > 1$. If the median redshift increases with limiting magnitude of the sample, then we can in principle expect to see this distinctive upturn at faint magnitudes.

It has been noted by Broadhurst (1996) that the reddest galaxies, as defined by $V-I$ colors, have a small number-count slope $s < 0.2$. Moreover, Broadhurst et al. (1996) have shown that the number-count slope is a decreasing function of $V-I$ color, i.e., red-selected samples have a shallower slope. Bearing this in mind, we define color-selected subsamples such that the slope of the number counts is 0.2. This was done as follows. For a given magnitude limit in R we arranged the galaxies in order of increasing $R-I$ color index. We removed blue galaxies until the slope of the number counts of the remaining sample was $s = 0.2$ and calculated $w(\theta)$ in the same way as for the full sample.

The results are shown in Figure 4 in the same form as in Figure 1, and are listed in columns (6)–(8) of Table 1. As for the full sample, we detect a correlation signal down to $R \sim 29$. Figure 5 is equivalent to Figure 3 for the full sample, except that there are no BSM data points, since they have no color-selected samples. The dotted curves are

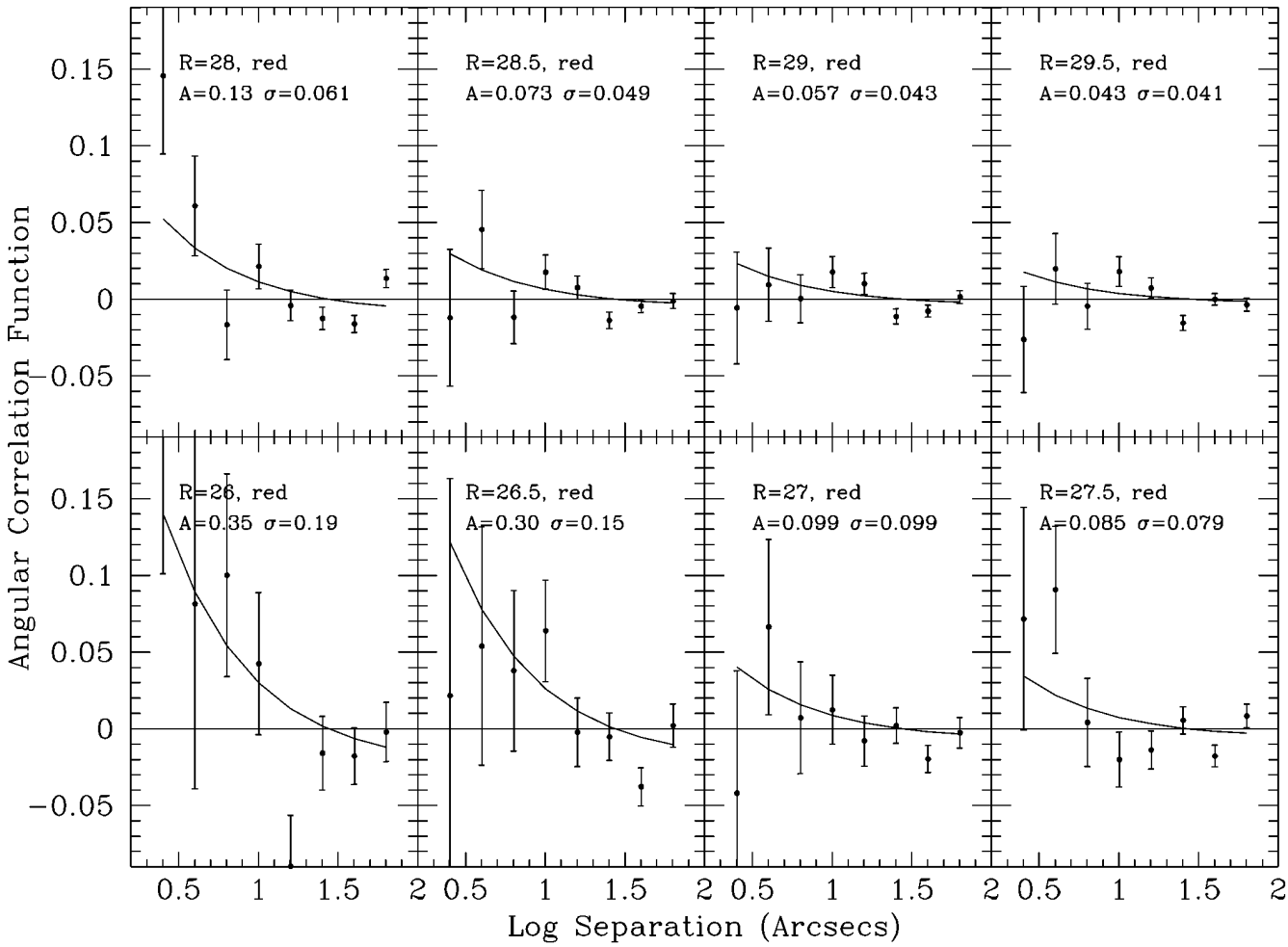

FIG. 4.—Measured $w(\theta)$ for the red-selected galaxies brighter than the limiting magnitude R as indicated in each panel. Error bars represent the 1 σ Poisson errors. The solid lines are the best fits for fixed power-law index $\gamma = 1.8$. The integral constraint (see text) has been subtracted from the fits.

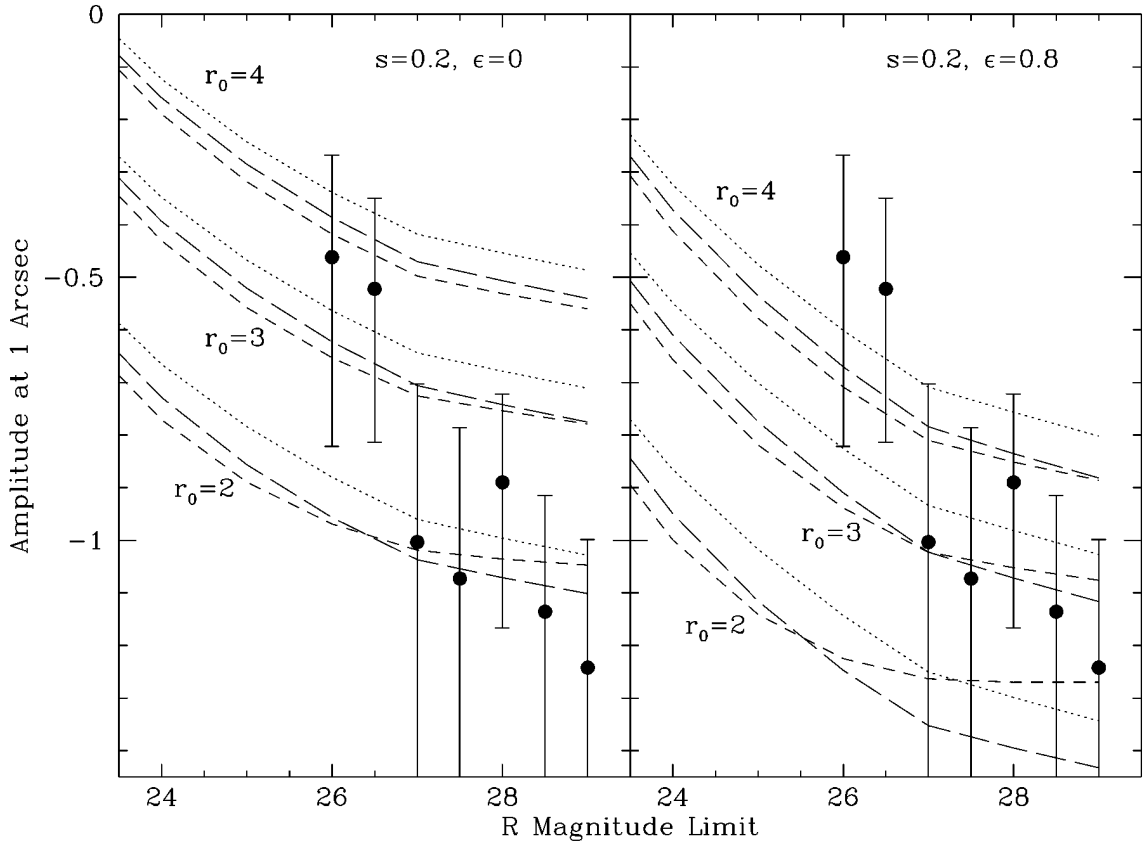

FIG. 5.—Observed amplitude of $w(\theta)$, measured at 1″ separation as a function of limiting R magnitude, for $24 < R < 29$ for the red-selected sample. The data points are from the HDF data sample only. The curves are theoretical predictions assuming $N(z)$ as described in the text for different values of the present correlation lengths r_0 as indicated. In the left-hand panel $\epsilon = 0$ is assumed, while in the right-hand panel $\epsilon = 0.8$ is assumed. The dotted curves are predictions without the effects of magnification bias. The dashed curves are equivalent curves including the effects of magnification bias. The long-dashed curves are for $\sigma_8 = 0.5$, and the short-dashed curves are for $\sigma_8 = 1$. The observed number-count slope $s = 0.2$ is used in the predictions.

the same for the full sample shown in Figure 3, as they do not include the magnification bias. We have assumed the same redshift distribution for the color-selected sample for illustrative purposes only. The two samples need not have the same redshift distribution. The dashed curves include the effects of magnification bias.

The theoretical predictions for the correlation amplitude show the expected larger influence of the magnification bias. The major differences in including the magnification bias for the red-selected sample are the following: (1) At brighter magnitudes, $R \lesssim 25$, the effect is significantly larger than for the full sample but has a similar behavior. (2) At faint magnitudes the effects are much more complicated. For $\sigma_8 = 0.5$ models, the observed effect of magnification bias for the color-selected sample is larger than for the full sample, but again not enough to significantly affect the conclusions about r_0 for a given ϵ. For $\sigma_8 = 1$ models, the behavior is quite different, with the curves flattening out and in some cases showing an upturn at faint magnitudes. Unfortunately, the upturn is not a generic feature but occurs only for models with weak intrinsic clustering. Furthermore, an upturn in the correlation amplitude at faint magnitudes could have other explanations, such as a very faint local population of galaxies.

It is important to note that the effects of magnification bias can be larger at brighter magnitudes than at fainter magnitudes. This is important, since it allows us to use spectroscopic information to measure the magnification bias. There are several ways of implementing this process. If we have some redshift information, either photometric or spectroscopic, physical pairs can be removed from the sample, and the observed $w(\theta)$ would be a direct measure of the magnification bias. An alternative way is having spectroscopic redshifts for a random subsample so that we can derive $N(z)$ and $\xi(r, z)$ directly. From this information we can compute the true $w(\theta)$ from Limber's equation and compare this result with the measured $w(\theta)$. The difference would then be the contribution from magnification bias, from which we can measure $\Omega_0\sigma_8$.

7. CONCLUSIONS

Analysis of the multicolor HDF data using the two-point angular correlation function leads us to the following conclusions:

1. We detect a clustering signal down to a magnitude limit of $R = 29$.

2. We find values of the amplitude of the $w(\theta)$ consistent with those obtained from ground-based observations at $R \sim 26$. The amplitude continues to decrease down to the faintest magnitude limit considered with a slope consistent with $\gamma \sim 1.8$.

3. Our results show that the measured amplitudes of $w(\theta)$ are consistent with some of the theoretical models. The

best-fit model is one with linear evolution of the correlation function, i.e., $\epsilon = 0.8$, and a present-day correlation length $r_0 \sim 4\,h^{-1}$ Mpc, similar to that observed for *IRAS* galaxies. This would be consistent with a large population of normal galaxies already being in place at $z \lesssim 1.7$.

4. We also show that even though magnification bias is expected to have an impact on the angular correlation function at faint magnitudes, it is not strong enough to affect seriously the conclusions about r_0 and ϵ, even for a red-selected sample, for which magnification bias should be more important.

5. The effects of magnification bias can be important for samples with a limiting magnitude of $R \lesssim 25$, which corresponds to the spectroscopic limit of large telescopes. This makes it possible to measure the effects of magnification bias and therefore get an alternative way of measuring $\Omega_0\sigma_8$. Given the estimates for the magnification bias, this requires a galaxy sample large enough to allow measurements of $w(\theta)$ to better than 10% accuracy.

Deep imaging and redshift surveys from ground-based telescopes will make it possible to draw more definite conclusions about the effects of magnification bias and its potential use for the measurement of Ω.

We would like to thank Warrick Couch for his HDF catalog of galaxies, and the ESO/ECF HDF group for many useful discussions.

REFERENCES

Barrow, J. D., Sonoda, D., & Bhavsar, S. P. 1984, MNRAS 210, 19
Bertin, E., & Arnouts, S. 1995, A&AS, 117, 393
Blandford, R. D., Saust, A., Brainerd, T. G., & Villumsen, J. V. 1991, MNRAS, 251, 600
Brainerd, T. G., Blandford, R. D., & Smail, I. 1996, ApJ, 466, 623
Brainerd, T. G., Smail, I. R., & Mould, J. R. 1995, MNRAS, 275, 781 (BSM)
Broadhurst, T. J. 1996, ApJ, in press
Broadhurst, T. J., Taylor, A. N., & Peacock, J. A. 1995, ApJ, 438, 49
Broadhurst, T. J., Villumsen, J. V., Smail, I., Charlot, S. 1996, in preparation
Charlot, S. 1996, private communication
Clements, D. L., & Couch, W. J. 1996, MNRAS, 280, L43
Cole, S., Ellis, R. S., Broadhurst, T. J., & Colless, M. M. 1994, MNRAS, 267, 541
Colley, W. N., Rhoads, J. E., Ostriker, J. P., & Spergel, D. N. 1996, preprint
Couch, W. J. 1996, private communication
Couch, W. J., Jurcevic, J. S., & Boyle, B. J. 1993, MNRAS, 260, 241
Efstathiou, G., Bernstein, G., Katz, N., Tyson, J. A., & Guhathakurta, P. 1991, ApJ, 380, L47
Fisher, K. B., Davis, M., Strauss, M. A., Yahil, A., & Huchra, J. 1994, MNRAS, 266, 50
Glazebrook, K., Ellis, R., Colless, M., Broadhurst, T., Allington-Smith, J., & Tanvir, N. 1995, MNRAS, 273, 157
Holtzman, J. A., Burrows, C. J., Casertano, S., Hester, J. J., Trauger, J. T.,Watson, A. M., & Worthey, G. 1996, ApJ, submitted
Landy, S. D., & Szalay, A. S. 1993, ApJ, 412, 64
Landy, S. D., Szalay, A. S., & Koo, D. C. 1996, ApJ, 460, 94
Le Fèvre, O., Hudon, D., Lilly, S. J., Crampton, D., Hammer, F., & Tresse, L. 1996, ApJ, 461, 534
Mobasher, B., Rowan-Robinson, M., Georgakakis, A., & Eaton, N. 1996, preprint
Neuschaefer, L. W., Windhorst, R. A., & Dressler, A. 1991, ApJ, 382, 32
Peebles, P. J. E. 1980, The Large-Scale Structure of the Universe (Princeton: Princeton Univ. Press)
Roche, N., Shanks, T., Metcalfe, N., & Fong, R. 1993, MNRAS, 263, 360
Smail, I., Hogg, D. W., Yan, L., & Cohen, J. G. 1995, ApJ, 449, L105
Stevenson, P. R., Shanks, T., Fong, R., & MacGillivray, H. T. 1985, MNRAS, 213, 953
Villumsen, J. V. 1996, MNRAS, submitted (V96)
Williams, R. E., et al. 1996, ApJ, submitted